The effect of surface roughness on the adhesion of solid surfaces for systems with and without liquid lubricant

V. N. Samoilov
Institut für Festkörperforschung (IFF), FZ-Jülich, 52425 Jülich, Germany
and Physics Faculty, Moscow State University, 117234 Moscow, Russia

I. M. Sivebaek
Institut für Festkörperforschung (IFF), FZ-Jülich, 52425 Jülich, Germany
and MEK-Energy, Technical University of Denmark, 2800 Lyngby, Denmark

B. N. J. Persson
Institut für Festkörperforschung (IFF), FZ-Jülich, 52425 Jülich, Germany

We present molecular dynamics results for the interaction between two solid elastic walls during pull-off for systems with and without octane (C_8H_{18}) lubricant. We used two types of substrate—flat and corrugated—and varied the lubricant coverage from ~1/8 to ~4 ML (monolayers) of octane. For the flat substrate without lubricant the maximum adhesion was found to be approximately three times larger than for the system with the corrugated substrate. As a function of the octane coverage (for the corrugated substrate) the pull-off force first increases as the coverage increases from 0 to ~1 ML, and then decreases as the coverage is increased beyond monolayer coverage. It is shown that at low octane coverage, the octane molecules located in the substrate corrugation wells during squeezing are pulled out of the wells during pull-off, forming a network of nanocapillary bridges around the substrate nanoasperities, thus increasing the adhesion between two surfaces. For greater lubricant coverages a single capillary bridge is formed. The adhesion force saturates for lubricant coverages greater than 3 ML. For the flat substrate, during pull-off we observe discontinuous, thermally activated changes in the number n of lubricant layers ($n-1 \rightarrow n$ layering transitions), whereas for the corrugated substrate these transitions are "averaged" by the substrate surface roughness. © *2004 American Institute of Physics.* [DOI: 10.1063/1.1806814]

I. INTRODUCTION

Tribology, the science of interacting solid surfaces in relative motion, has been studied intensively for many years. It is of great theoretical interest and involves fundamental physics, e.g., questions related to the origin of irreversibility, the role of self-organized criticality, and in the case of boundary lubrication, dynamical phase transitions in molecularly thin lubrication layers. In particular, squeezing of thin lubrication or contamination layers has attracted much attention (see Refs. 1–5).

Even a highly polished surface has surface roughness on many different length scales. When two bodies with nominally flat surfaces are brought into contact, the area of real contact will usually only be a small fraction of the nominal contact area.[6] We can visualize the contact regions as small areas where asperities from one solid are squeezed against asperities of the other solid.

The influence of surface roughness on the adhesion between elastic solid and a hard substrate has been studied in a classical paper by Fuller and Tabor.[7] They found that already a relatively small surface roughness can remove the adhesion. In order to understand the experimental data they developed a very simple model based on the assumption of surface roughness on a single length scale. The overall contact force was obtained by applying the JKR contact theory[8] to each individual asperity.

A more general theory of adhesion between randomly rough surfaces was presented in Ref. 9 (see also Refs. 10–12) and adhesion of elastic bodies both with and without account for surface roughness was thoroughly investigated recently (see Refs. 9–17).

Adhesion plays an important role in many applications.[18] Biological systems are examples of these.[16,17] Furthermore it has been shown that adhesion has an influence on sliding friction.[19] This expands the importance of adhesion significantly.

We have presented several computer simulations of boundary lubrication for realistic model systems characterized by different (realistic) parameters (see Refs. 20 and 21–27). For other studies involving squeezing of alkanes, see Refs. 28–33. When two elastic solids with curved and atomically smooth surfaces are squeezed together in a fluid which wets the solid walls, a small asperity contact region is formed, where the surfaces are parallel and separated by an integer number of monolayers of trapped lubricant fluid. For this case it has been shown both experimentally and theoretically that when quasispherical and linear hydrocarbons are confined between atomically flat surfaces at microscopic separations, the behavior of the lubricant is mainly determined by its interaction with the solid walls that induces layering in the perpendicular direction.[3,34–40] The thinning of the lubrication film occurs stepwise, by expulsion of indi-
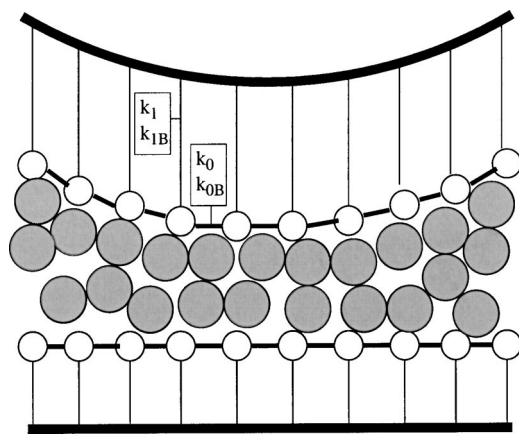
FIG. 1. Schematic picture of the central region of the adhesion model used in the present article.

vidual layers. These layering transitions appear to be thermally activated (see Refs. 41 and 42).

In Ref. 22 we have studied the adhesion force, and the $n-1 \rightarrow n$ layering transition during pull-off, for elastic solids with smooth surfaces. In the present paper, we focus on the influence of surface roughness (on two length scales) and thin lubricant or contamination films, on the adhesion between two surfaces.

II. THE MODEL

The model was described in Refs. 21, 22, and 24, but we review it briefly here. We are concerned with the properties of a lubricant film squeezed between the curved surfaces of two elastic solids. In experiments, a system of this type is obtained by gluing two elastic slabs (of thickness W_1 and W_2) to "rigid" surface profiles of arbitrary shape. If the radii of curvature of the rigid surfaces are large compared to W_1 and W_2, the elastic slabs will deform, reproducing with their free surfaces the (nearly arbitrary) shape of the underlying rigid profiles.

In what follows we denote the lower solid as *substrate*, which is taken to be fixed in space. The upper solid, denoted as *block*, will be moving. To account for the elastic response of the slabs, without dealing with the large number of atoms required to simulate a mesoscopic elastic solid we treat explicitly, at the atomistic level, only the last atomic layer of the solids at the interface. These atoms are connected to a *rigid* curved surface (or profile). The force constants connecting these atoms to the rigid profile, however, are not the bare parameters, determined by the model interatomic potential. Instead, those force constants are treated as effective parameters that implicitly reintroduce the elastic response of the slabs of arbitrary thickness W_1 and W_2.

The model is illustrated in Fig. 1 (see also Refs. 21 and 22). The atoms in the bottom layer of the block (open circles) form a simple square lattice with lattice constant a, and lateral dimensions $L_x = N_x a$ and $L_y = N_y a$. In the following, periodic boundary conditions are assumed in the xy plane. The atoms interact with each other via "stiff" springs (thick lines) and execute bending and stretching motion characterized by a bending force constant k_{0B} and a stretching force

constant k_0, respectively. Moreover, each atom is connected to the upper rigid surface profile by "soft" elastic springs (thin lines) of bending force constant k_{1B} and stretching force constant k_1. As described in Refs. 21 and 22, the numerical values of all these force constants k_0, k_{0B}, k_1, and k_{1B} are determined in such a way as to mimic the elastic response of the entire slab.

The substrate is treated in a similar way as the block, but we use slightly different lattice constant in order to avoid having (low order) commensurate structures formed at the interface. The space between the block and the substrate is occupied by a layer (monolayer or more) of the lubrication fluid (full circles in Fig. 1).

The molecular dynamics calculations have been performed by keeping the temperature of the solid walls fixed at their outer boundaries (see Ref. 21). This is a realistic treatment, and it implies that heat flows from the lubricant to the confining walls. In the present calculations the temperature of the solid walls was always equal to 300 K.

Below we study mainly the average pressure. The pressure acting on a wall atom is defined as the total normal force acting on the wall atom from the lubricant atoms and from the other wall, divided by the area a^2. The average pressure is the z component of the total force acting on the solid block from the lubricant and the substrate, divided by the total area $L_x \times L_y$.

Below we provide details of the models used for the block, the substrate, and the lubricants in the simulations carried out in the present work, which differ from those described in Refs. 21 and 22.

Both solids, the block and the substrate, were gold. We used the same elastic modulus and Poisson ratio for the block and the substrate, which were $E = 7.72 \times 10^{10}$ Pa and $\nu = 0.42$ for gold. We used systems with two types of substrates—atomically flat and "nanocorrugated" (see details below). In the case of the system with flat substrate we used the same thickness for the block and the substrate $W = 50$ Å. This choice of thicknesses implies that the block and the substrate used in our simulations will deform elastically similar to each other. In the case of the system with corrugated substrate we used the substrate thickness $W_1 = 10$ Å and the block thickness $W_2 = 90$ Å. In the simulations we used a system of lateral dimensions $L_x = 506$ Å and $L_y = 75.9$ Å. For the substrate we used $N_x = 200$ and $N_y = 30$ atoms in the x and y directions, forming a square lattice with lattice constant $a = 2.53$ Å. The corresponding parameters for the block were $N_x = 180$, $N_y = 27$, and $a = 2.81$ Å.

The block rigid profile was taken to be cosine corrugated in the x direction, with corrugation amplitude (difference between maximal and minimal surface heights) $0.1 L_x$ and wavelength L_x. We used two types of substrate corrugations—atomically flat surface and nanocorrugated surface. In the latter case the rigid substrate profile had a sine corrugation of the form

$$h(x,y) = h_0 \sin(2\pi x/\lambda_x) \sin(2\pi y/\lambda_y), \tag{1}$$

with roughness amplitude $h_0 = 5$ Å and the wavelengths $\lambda_x = L_x/13$ and $\lambda_y = L_y/2$. Thus we studied the effect of corru-

gation (nanoroughness) of the substrate on the confined lubricant structure and adhesion of two surfaces during retraction.

Octane lubricant C_8H_{18} was used in the present calculations. It was chosen as having an intermediate chain length (and properties) among the linear alkanes of different chain lengths C_3H_8, C_4H_{10}, C_8H_{18}, C_9H_{20}, $C_{10}H_{22}$, $C_{12}H_{26}$, and $C_{14}H_{30}$, lubricating properties of which have been considered recently in Refs. 24–26. The lubricating properties of octane have also been studied recently in Ref. 27. We considered C_8H_{18} chain molecules consisting of eight beads in the united atom representation. The Lennard-Jones potential was used to model the interaction between beads of different chains:

$$v(r) = 4\epsilon_0 \left[\left(\frac{r_0}{r} \right)^{12} - \left(\frac{r_0}{r} \right)^6 \right], \tag{2}$$

and the same potential with modified parameters (ϵ_1, r_1) was used for the interaction of each bead with the substrate and block atoms. For the interactions within the C_8H_{18} we used the OPLS model (Refs. 43 and 44), including flexible bonds, bond bending, and torsion interaction, which results in bulk properties in good agreement with experimental data. The parameters were $\epsilon_0 = 5.12$ meV for the both interior and end beads, and $r_0 = 3.905$ Å in all cases. Atomic mass 14 (for interior CH_2 beads) and 15 (for the CH_3 end groups) were used. For the interaction of each bead with the substrate and block atoms we took $\epsilon_1 = 18.60$ meV and $r_1 = 3.28$ Å.[45] The latter choice reflects stronger interaction between the beads and metal surfaces than between the bead units of different lubricant molecules. For these parameters octane is wetting both metal surfaces (see also Ref. 27).

Within a C_8H_{18} chain we assume nearest neighbor C atoms are connected via springs with the spring constant k, which was chosen equal to 10 N/m. Time step was equal to 1 fs. We used an angle bending interaction of the form $E(\cos\theta)/k_B = 1/2 k_{bend}(\cos\theta - \cos\theta_0)^2$ with $k_{bend} = 62\,543$ K and $\theta_0 = 2.0001$ rad.[44] For the dihedral interaction we used the functional form in terms of a cosine Fourier series $E(\phi)/k_B = \Sigma_{i=0}^3 c_i \cos^i(\phi)$ with parameters $c_0 = 1009.99$ K, $c_1 = 2018.95$ K, $c_2 = 136.37$ K, and $c_3 = -3165.30$ K.[44] Internal beads of separation greater than three units were treated similarly as beads from different chains.

For interaction between atoms of the block and the substrate we used the Lennard-Jones potential with the parameters $\epsilon_{12} = 18.60$ meV and $r_{12} = 3.28$ Å, the same as used in Ref. 24.

To study the effect of thin contamination or lubricant layers on the interaction between two surfaces during retraction we changed the number of octane molecules in the system from 0 to 2364 molecules, corresponding to ~4 ML of octane in the contact region. We studied the systems without lubricant and with ~1/8, 1/4, 1/2, 1, 2, 3, and 4 ML of octane in the contact region.
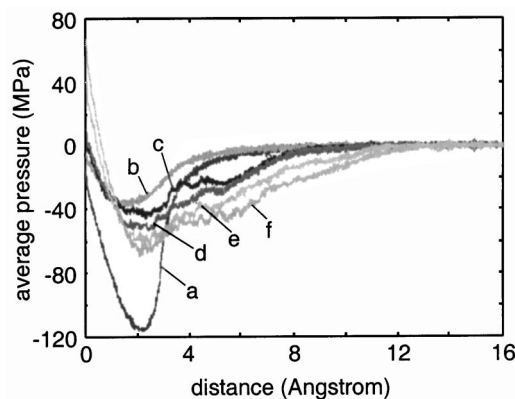

FIG. 2. The variation of the average pressure during retraction developed as the block moves a distance of 16 Å away from the substrate. Octane C_8H_{18} was used as lubricant. Pull-off (retraction) velocity was $v_z = 1$ m/s. (a) For the flat substrate without lubricant. (b) For the corrugated substrate without lubricant. Curves (c)–(f) show results for the corrugated substrate with about 1/8, 1/4, 1/2, and 1 ML of octane in the contact region, respectively. For clarity, the curve for the flat substrate (a) is displaced to the right, by 2 Å.

III. SIMULATION RESULTS AND DISCUSSION

We now describe the results obtained from our simulations for octane C_8H_{18} squeezed between two solid elastic walls for different lubricant coverages in the contact region.

Let us first discuss the results obtained for the corrugated substrate and relatively low octane coverage in the contact region. Figure 2 shows the variation of the average pressure during retraction as the block moves a distance of 16 Å away from the substrate. The pull-off (retraction) velocity was $v_z = 1$ m/s. We have varied the lubricant coverage from 0 to 1 ML in the contact region. We will demonstrate below that the adhesion (attraction) between the block and the corrugated substrate with molecular thin lubrication or contamination films is due to the formation of (capillary) "nanobridges" between the block and the nanoasperities of the substrate. The pull-off force is maximal when the adsorbate coverage is of the order of 1 ML [curve (f)]. However, the pull-off force is still smaller than for a flat substrate without lubricant [curve (a)].

For the corrugated substrate, increase of the lubricant coverage in the contact region results in an initial increase of the pull-off force, see curves (b)–(f), and in the shift of the pull-off point toward greater distances. Note also that with lubricant the adhesion between the surfaces is observed at larger separations due to formation of a "large" capillary bridge in the center of the contact region, see curves (b)–(f). In all cases the pull-off force is reduced compared to the smooth surface (a). The pull-off force for the flat substrate without lubricant is approximately three times larger than for the system with the corrugated substrate.

The pull-off force will in general depend on the retraction velocity. A few test calculations were performed at lower and higher pull-off velocities in order to reveal the effect of retraction velocity on the average pressure vs distance curves. Figure 3 shows the variation of the average pressure during retraction as the block moves a distance of 16 Å away from the substrate for the corrugated substrate with about 1/2 ML of octane in the contact region. The pull-off (retraction)
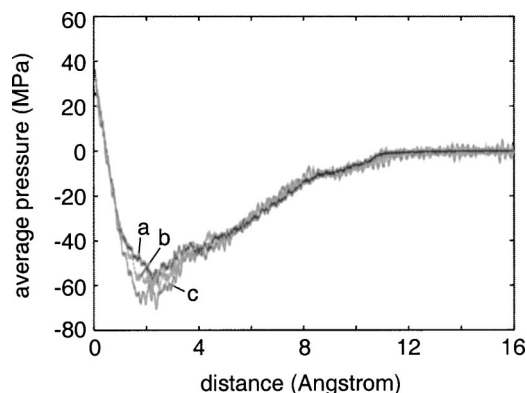
FIG. 3. The variation of the average pressure during retraction developed as the block moves a distance of 16 Å away from the substrate. Octane C_8H_{18} was used as lubricant. For the corrugated substrate with ~1/2 ML of octane in the contact region. Pull-off (retraction) velocity was $v_z = 0.1$ m/s (a), $v_z = 1$ m/s (b), and $v_z = 5$ m/s (c).

velocity was $v_z = 0.1$ m/s (a), $v_z = 1$ m/s (b), and $v_z = 5$ m/s (c). A small decrease of the pull-off force is observed with the decrease of the pull-off velocity, but the values obtained for velocities $v_z = 0.1$ m/s and $v_z = 1$ m/s are close to each other indicating that no new physics may be expected with lower pull-off velocities.

Let us now discuss the nature of the adhesion for the corrugated substrate, with ~1/4 ML of octane in the contact region. In Fig. 4 we show snapshot pictures of the lubricant layer during retraction, as the block moves away from the substrate for three different block positions $d = 0$, 3, and 6 Å. Only the central part of the contact between the block and the substrate is shown, top view, after removing the block and substrate atoms. In the beginning ($d = 0$ Å) octane molecules are located in the substrate corrugation wells, or cavities with direct metal-metal contact between the block and the top of the substrate nanoasperities. During retraction ($d = 3$ Å) the octane molecules are pulled out of the wells forming an almost symmetric network of nanobridges around the asperity tops, increasing the adhesion between the two surfaces. This configuration corresponds to the maximal adhesion force, see curve (d) in Fig. 2. Thus maximal adhesion is achieved via the formation of many small capillary nanobridges, involving just a few molecules for each bridge. Further retraction ($d = 6$ Å) results in the collapse of the nanobridges and the formation of a single large capillary bridge in the center of the contact region.

In Fig. 5 we show snapshot pictures (for six different block positions) during retraction for the same system as in Fig. 4 but including the atoms (unfilled circles) of the bottom surface of the block and the top atoms of the substrate. We show the side view of the central 108 Å×50 Å section (in the x-y plane) of the contact area. For $d = 2$ Å the contact area between the block and the substrate (through the lubricant) is the largest. This configuration corresponds to the maximal adhesion force, see curve (d) in Fig. 2. In the beginning ($d = 0$ Å) the octane molecules are located in the substrate corrugation wells, with direct metal-metal contact between the block and the substrate at the asperity tops. During retraction ($d = 2$ Å and 4 Å) the octane molecules are
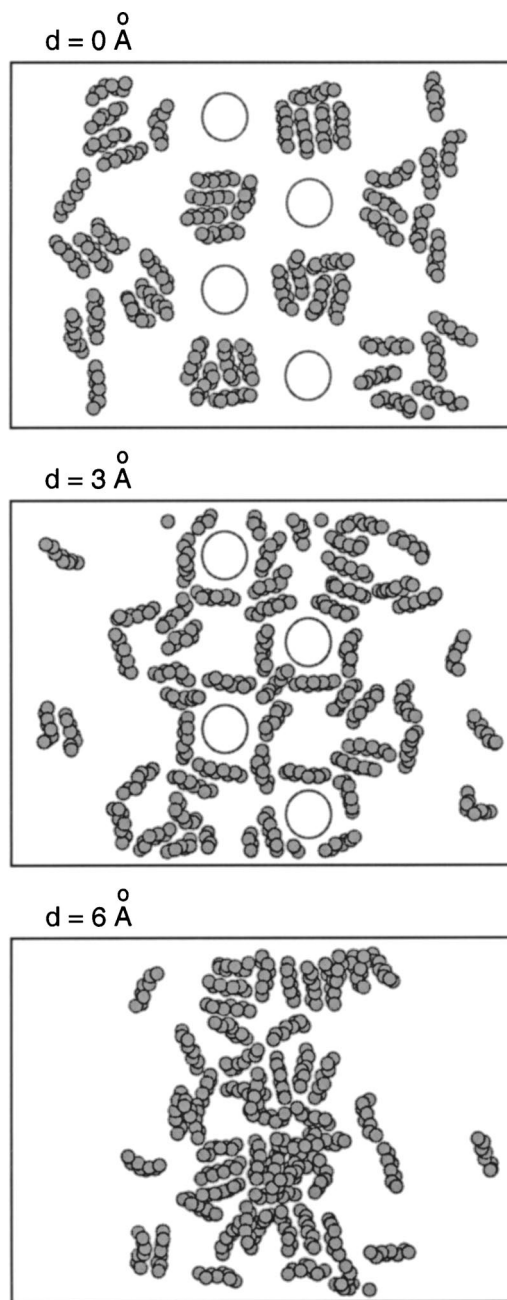

FIG. 4. Snapshot pictures (for three different block positions $d = 0$, 3, and 6 Å) of the lubricant layer during retraction. We only show the central part of the contact between the block and the substrate. Top view, after removing the block and substrate atoms. Octane C_8H_{18} was used as lubricant. Pull-off (retraction) velocity was $v_z = 1$ m/s. For the corrugated substrate with ~1/4 ML of octane in the contact region. The circles indicate the position of several asperity tops of the corrugated substrate surface.

pulled out of the wells, forming nanobridges which increase the adhesion between the two surfaces. Further retraction results in return of the lubricant molecules to the substrate corrugation wells ($d = 6$ Å) and the formation of a large capillary bridge in the center of the contact region.

In Fig. 6 we show snapshot pictures (for seven different block positions) during retraction, as the block moves away from the substrate for the system with the corrugated substrate with ~1 ML of octane in the contact region. The snapshot pictures show the side view of the central 170 Å×50 Å
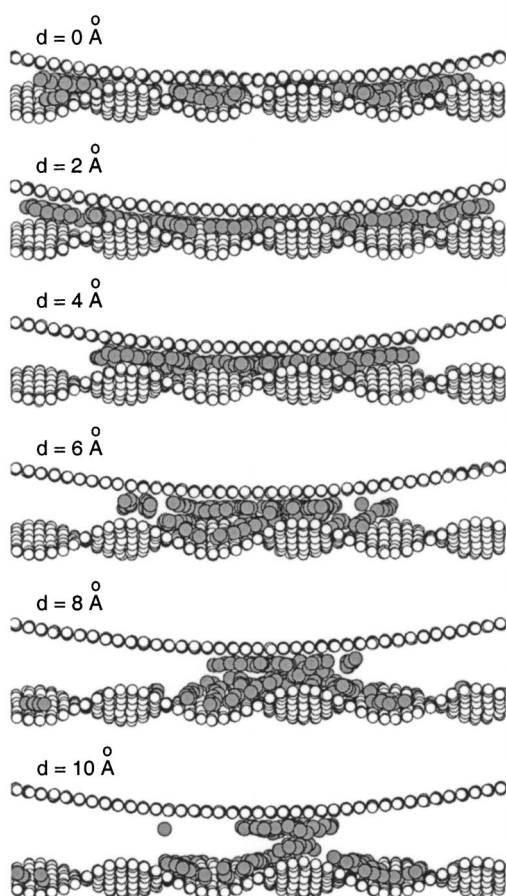
FIG. 5. Snapshot pictures (for six different block positions) during retraction. The snapshot pictures show the side view of the central 108 Å×50 Å section (in the x-y plane) of the contact area. Octane C_8H_{18} was used as lubricant. Pull-off (retraction) velocity was $v_z = 1$ m/s. For the corrugated substrate with ~1/4 ML of octane in the contact region.
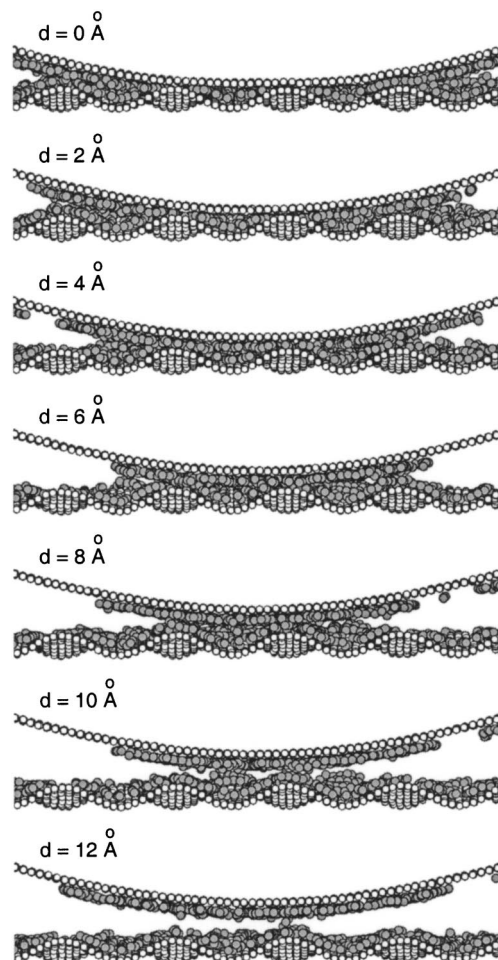

FIG. 6. Snapshot pictures (for seven different block positions) during retraction. The snapshot pictures show the side view of the central 170 Å×50 Å section (in the x-y plane) of the contact area. Octane C_8H_{18} was used as lubricant. Pull-off (retraction) velocity was $v_z = 1$ m/s. For the corrugated substrate with ~1 ML of octane in the contact region.

section (in the x-y plane) of the contact area. In the beginning ($d = 0$ Å) octane molecules are again located in the substrate corrugation wells, with direct metal-metal contact between the block and the substrate at the asperity tops. The lubricant is under high pressure in the central part of the contact area, squeezed between the two elastic metal surfaces. Thus, a strong repulsive force is acting on the block corresponding to high positive average pressure, see curve (f) in Fig. 2 at $d = 0$ Å. For this block position the contact area between the block and the substrate (through the lubricant) is the largest. For $d = 2$ Å the contact area is a bit less, but the adhesion force is maximal, see curve (f) in Fig. 2. During further retraction ($d = 4$ and 6 Å), the octane molecules form well defined monolayers contacting both the block surface and the substrate surface (in the substrate corrugation wells) with vacant gaps in between them. The latter is due to the stronger interaction (attraction) between the beads of lubricant molecules and metal surfaces than between the bead units of different lubricant molecules, as the (realistic) parameters used in the present calculations were $\epsilon_0 = 5.12$ meV and $\epsilon_1 = 18.60$ meV. Thus lubricant molecules form many small capillary nanobridges at the corrugated substrate tops, see snapshots at $d = 8$ and 10 Å. Due to higher lubricant coverage in the contact region, there are enough

octane molecules to form capillary nanobridges without being pulled out of the wells, as was the case for low lubricant coverage (~1/4 ML of octane in the contact region). Thus adhesion for higher lubricant coverage is also governed by the mechanism of formation of small capillary nanobridges but with some new features.

Let us contrast the results presented above with the adhesion with the corrugated and flat substrates without lubricant. In this case the adhesion is due to direct metal-metal interaction (attraction) between the block and the substrate, and the adhesion force depends on the area of real contact, which is different for the systems with the corrugated and the flat substrates.

In Fig. 7 we show snapshot pictures (for four different block positions $d = 0$, 1, 2, and 3 Å) during retraction, as the block moves away from the substrate for the system with the corrugated substrate without lubricant. The snapshot pictures show the side view of the central 108 Å×50 Å section (in the x-y plane) of the contact area. In the beginning ($d = 0$ Å) strong repulsion is observed and manifested in the figure by the visible deformations of the block profile. Other surface areas, where the atoms of two surfaces are located at
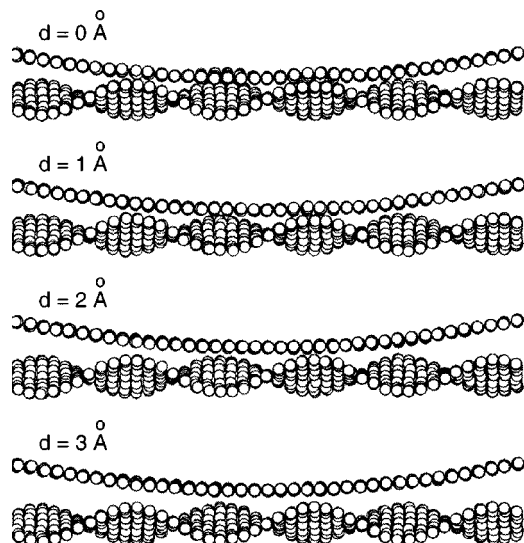
FIG. 7. Snapshot pictures (for four different block positions) during retraction. The snapshot pictures show the side view of the central 108 Å×50 Å section (in the x-y plane) of the contact area. Pull-off (retraction) velocity was $v_z = 1$ m/s. For the corrugated substrate without lubricant.

FIG. 9. The variation of the average pressure during retraction developed as the block moves a distance of 16 Å away from the substrate. Octane C_8H_{18} was used as lubricant. Pull-off (retraction) velocity was $v_z = 1$ m/s. For the corrugated substrate. Curves (a)–(d) correspond to ~ 1, 2, 3, and 4 ML of octane in the contact region, respectively.

greater distances, interact attractively. Thus the average pressure is negative, see curve (b) in Fig. 2. During retraction ($d = 1$ and 2 Å), the repulsion resulting from the spots of direct contact between two surfaces decreases. The latter configuration corresponds to the maximal adhesion force. Further retraction ($d = 3$ Å) results in the decrease of the adhesion force between the two surfaces.

In Fig. 8 we show snapshot pictures (for the block displacements $d = 0$, 1, 2, and 3 Å) during retraction for the flat substrate without lubricant. The snapshot pictures show the side view of the central 108 Å×50 Å section (in the x-y plane) of the contact area. In the beginning ($d = 0$ Å) strong repulsion arises from the area of direct contact, demonstrated by the visible deformation of the block profile. Other areas, where the atoms of two surfaces are located at greater distances, interact attractively. Thus the average pressure is negative, see curve (a) in Fig. 2. During retraction ($d = 1$ and
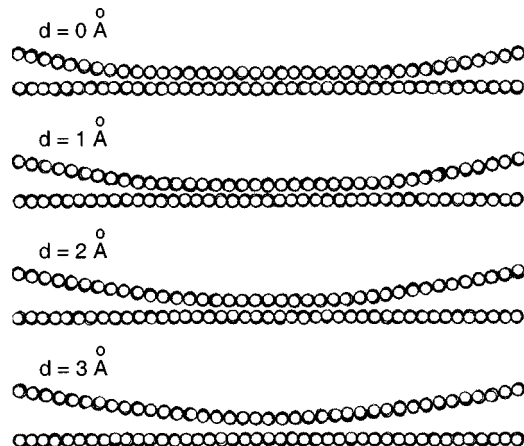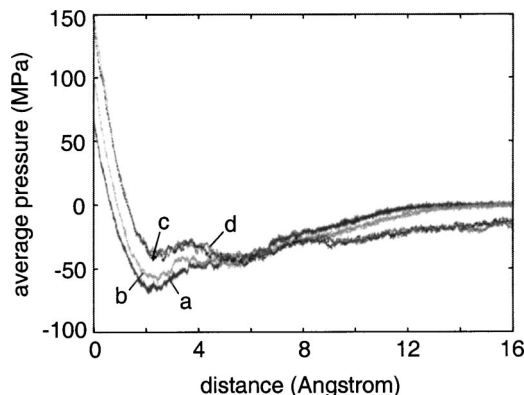
2 Å) the repulsion in the central area of direct contact decreases, corresponding to the elastic relaxation of the block profile (see Fig. 8). The latter configuration corresponds to the maximal adhesion force. The area of contact between the two bodies is much larger in this case, compared with that for the corrugated substrate (see Fig. 7). This results in approximately three times larger pull-off force for the flat substrate case. Further retraction ($d = 3$ Å) results in the sharp decrease of the adhesion force between the two surfaces. Thus we conclude that the short length scale corrugation (present in the system shown in Fig. 7) results in approximately three times decrease of adhesion force. When roughness occur on more length scales, the pull-off force will be even smaller.

We have shown that the pull-off force for rough surfaces increases when the thickness of the lubricant film increases from 0 to ~ 1 monolayer (see Fig. 2). We now address how the adhesion changes with further increase of the lubricant coverage in the contact region. Figure 9 shows the variation of the average pressure during retraction for the corrugated substrate with higher lubricant coverages. The lubricant coverage increases from ~ 1 ML [curve (a)] to 4 ML [curve (d)] of octane. Note that the maximal adhesion force decreases with the increase of the lubricant coverage, which is opposite to the increase observed in Fig. 2 for systems with small lubricant coverages. Some "saturation" of the adhesion force is observed for lubricant coverages greater than 3 ML, compare curves (c) and (d). We also note that in the beginning ($d = 0$ Å) a strong repulsion is observed between the block and the substrate corresponding to high positive average pressure, see curves (a)–(d). Here, the lubricant is under high pressure in the central part of the contact area, squeezed between the two elastic surfaces. Thus the increase of octane coverage in the contact region results in more octane molecules trapped in the substrate corrugation wells during squeezing and to the observed increase of repulsion between two metal surfaces at $d = 0$ Å. The other peculiarity observed is the inversion of the average pressure for distances greater than $d \sim 6$ Å with increasing the lubricant coverage in the contact region. This is due to the formation of "longer" cap-

FIG. 8. Snapshot pictures (for four different block positions) during retraction. The snapshot pictures show the side view of the central 108 Å×50 Å section (in the x-y plane) of the contact area. Pull-off (retraction) velocity was $v_z = 1$ m/s. For the flat substrate without lubricant.
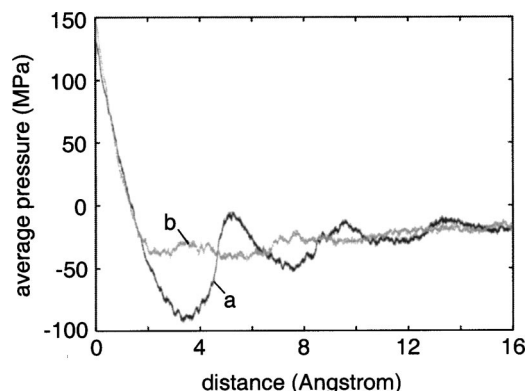
FIG. 10. The variation of the average pressure during retraction developed as the block moves a distance of 16 Å away from the substrate. Octane C_8H_{18} was used as lubricant. Pull-off (retraction) velocity was $v_z = 1$ m/s. For the flat substrate (a), and the corrugated substrate (b), in both cases with ~4 ML of octane in the contact region. The $n-1 \rightarrow n$ layering transitions are observed for the system with the flat substrate.
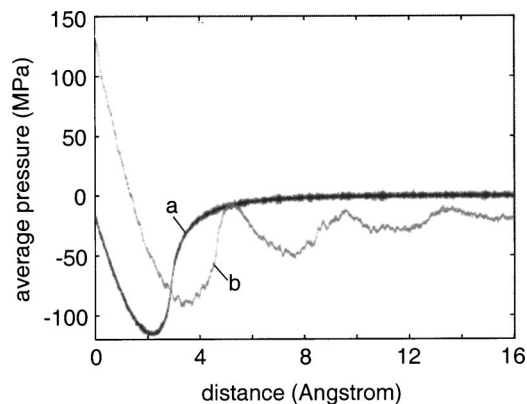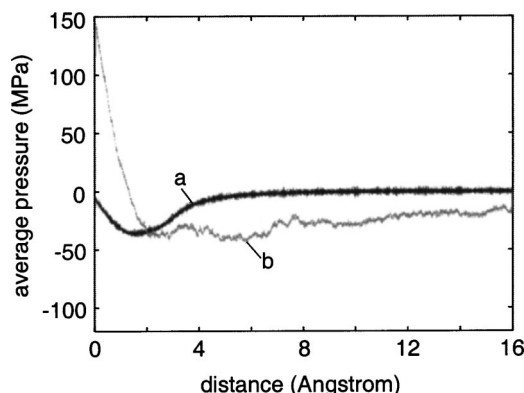

FIG. 12. The variation of the average pressure during retraction as the block moves a distance of 16 Å away from the substrate. Octane C_8H_{18} was used as lubricant. Pull-off (retraction) velocity was $v_z = 1$ m/s. For the corrugated substrate without lubricant (a), and with ~4 ML of octane in the contact region (b).

illary bridge for the system with higher octane coverage. The feature that during retraction the stress remains finite even at large strains was observed for high lubricant coverage and rough walls in Ref. 46.

Let us now compare the adhesion for the systems with the flat and the corrugated substrates for the case of high lubricant coverage. Figure 10 shows the variation of the average pressure during retraction for the flat and the corrugated substrates, in both cases with ~4 ML of octane in the contact region. The $n-1 \rightarrow n$ layering transitions are observed for the system with the flat substrate, whereas for the corrugated substrate these transitions are averaged out by the substrate surface roughness. Note the decrease of the maximal adhesion force for the corrugated substrate; the physical reason for this is different from the decrease observed in Fig. 2 for systems without lubricant. For the flat substrate with 4 ML of octane the average pressure drops down (the adhesion force increases) significantly before the $n-1 \rightarrow n$ layering transition (with $n=2$), see minimum of the curve (a) in Fig. 10 at $d \sim 3.5$ Å. When the $n=2$ monolayer is retracted the

average pressure relaxes almost to the zero level. The same behavior is observed also for the $n-1 \rightarrow n$ layering transitions for $n=3$ and 4. Thus the difference between the maximal adhesion forces observed for the flat and the corrugated substrates is now governed by the difference in retraction of monolayers of octane in the contact area during the pull-off. The peculiarity that the roughness slightly lowers the yield stress (maximal adhesion force) during retraction was observed in Ref. 46 but for much more long chain molecules used as lubricant.

Figure 11 shows the variation of the average pressure during retraction for the flat substrate without lubricant [curve (a)], and with ~4 ML of octane in the contact region [curve (b)]. The $n-1 \rightarrow n$ layering transitions are observed for the system with 4 ML of octane in the contact region. Comparison of the curves (a) and (b) shows that in frames of the present model the maximal adhesion force is greater for the system without lubricant. Due to the formation of the capillary bridge the adhesion (attraction) between the surfaces extends to much greater separations for the lubricated contact region.

Figure 12 shows the variation of the average pressure during retraction for the corrugated substrate without lubricant [curve (a)], and with ~4 ML of octane in the contact region [curve (b)]. The maximal adhesion force is slightly greater for the system with lubricant. The adhesion (attraction) between the surfaces extends to much greater separations between the block and the substrate in the case of the system with 4 ML of octane in the contact region due to formation of the capillary bridge. The latter feature is similar to that observed for the flat substrate in Fig. 11.

Finally, we consider the hysteresis of the average pressure vs distance dependence during squeezing and retraction. Figure 13 shows squeezing-retraction average pressure vs distance hysteresis curves for the corrugated substrate with about 1/8, 1/4, 1/2, and 1 monolayer of octane in the contact region. Curve (a) shows the variation of the average pressure during squeezing, and curve (b)—during retraction. The squeezing and retraction velocity was 1 m/s. The hysteresis

FIG. 11. The variation of the average pressure during retraction as the block moves a distance of 16 Å away from the substrate. Octane C_8H_{18} was used as lubricant. Pull-off (retraction) velocity was $v_z = 1$ m/s. For the flat substrate without lubricant (a), and with ~4 ML of octane in the contact region (b). The $n-1 \rightarrow n$ layering transitions are observed for the system with 4 ML of octane in the contact region.
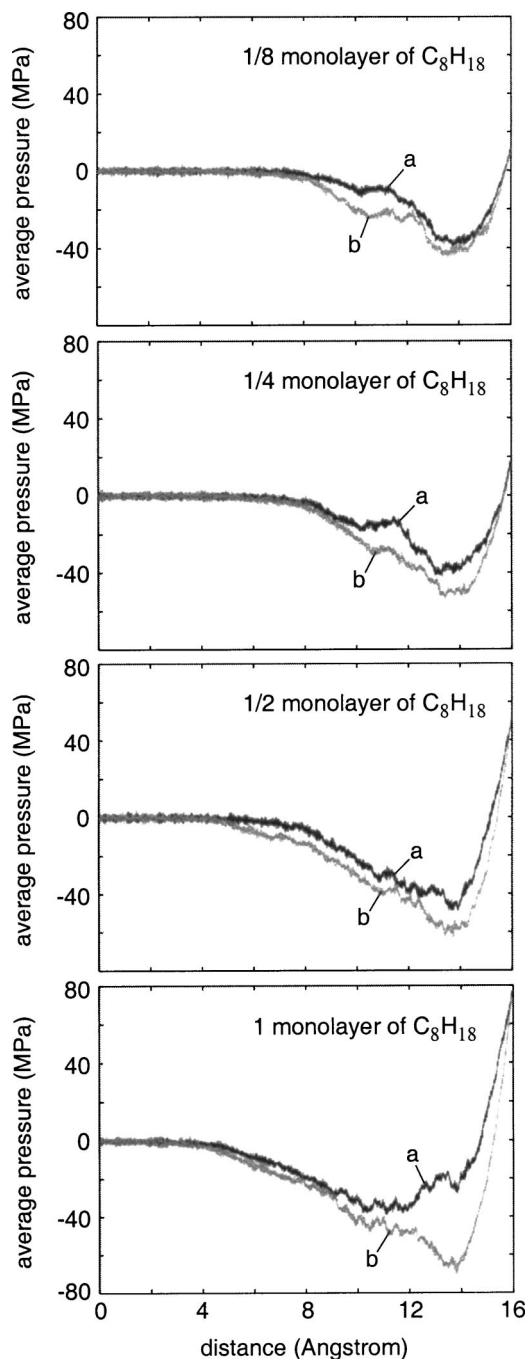
FIG. 13. Squeezing-retraction average pressure vs distance hysteresis curves. The variation of the average pressure during squeezing (*a*) and retraction (*b*) as the block moves a distance of 16 Å toward the substrate (*a*) and away from the substrate (*b*). Octane C_8H_{18} was used as lubricant. The squeezing and retraction velocity was 1 m/s. For the corrugated substrate with ~1/8, 1/4, 1/2, and 1 ML of octane in the contact region.

becomes more pronounced with the increase of the lubricant coverage.

IV. SUMMARY AND CONCLUSION

In this paper we have studied the adhesion between two rough solid elastic walls lubricated by octane. We used two types of substrates—flat and corrugated—and varied the lubricant coverage from ~1/8 to ~4 ML of octane. As a function of the octane coverage (for the corrugated substrate) the

pull-off force first increases as the coverage increases from 0 to ~1 ML, and then decreases as the coverage is increased beyond monolayer coverage. At low octane coverage, the octane molecules located in the substrate corrugation wells during squeezing are pulled out of the wells during pull-off, forming a network of nanocapillary bridges around the substrate nanoasperities, thus increasing the adhesion between two surfaces. For greater lubricant coverages a single capillary bridge is formed. The adhesion force saturates for lubricant coverages greater than 3 ML.

The present drive toward miniaturization of moving mechanical systems, e.g., micromotors, requires a better understanding of the role of adhesion and friction. The increased surface/volume ratio in small systems makes them more sensitive to adhesion and friction, and sometimes these forces are so high that the objects cannot slide or rotate on the solid substrate surface. Most surfaces have at least nanoscale roughness, and hard solids in the normal atmosphere have at least a monolayer of liquidlike "contamination" molecules, e.g., water and hydrocarbons. Thus, the study of adhesion presented in this paper should be relevant for many practical systems, particularly for small mechanical systems.

For clean surfaces the adhesion is largest for smooth surfaces. Surface roughness has two effects. First, surface roughness lowers the area of real contact. Since the adhesion interaction comes almost entirely from the area where the solids make atomic contact, it is clear that the surface roughness may drastically reduce the adhesion. Second elastic deformation energy is stored in the vicinity of the asperity contact regions. During pull-off the elastic energy is "given back" to the system, usually resulting in a drastic reduction in the effective adhesion and the pull-off force.

Small amount of lubricant or contamination liquids between rough solid walls may drastically enhance the adhesion. We have found in this study that (up to) a monolayer of a wetting liquid may result in the formation of a large number of nanobridges between the solids, which increases the pull-off force. This effect is well known experimentally. For example, the adhesion force which can be detected between gauge blocks (steel blocks with very smooth surfaces) is due to the formation of many very small capillary bridges made of water or organic contamination. For thicker lubrication or contamination films the effective adhesion will be more long ranged but the pull-off force may be smaller, as indeed observed in this study. The thickness of the lubricant or contamination layer for which the pull-off force is maximal will in general depend on the nature of the surface roughness. Some insects such as flies or crickets inject a thin layer of a wetting liquid in the contact region between the insect attachment surfaces and the (rough) substrate. The optimum amount of injected liquid will depend on the nature of the substrate roughness, and it is likely that the insect can regulate the amount of injected liquid by a feedback system involving the insect nerve system.

[1] B. N. J. Persson, *Sliding Friction: Physical Principles and Applications* (Springer, Heidelberg, 2000).

[2] B. N. J. Persson, Surf. Sci. Rep. **33**, 83 (1999).

[3] J. N. Israelachvili, *Intermolecular and Surface Forces* (Academic, London, 1995).

[4] J. Krim, Sci. Am. **275**, 74 (1996).

[5] J. Krim, Surf. Sci. **500**, 741 (2002).

[6] J. A. Greenwood and J. B. P. Williamson, Proc. R. Soc. London, Ser. A **295**, 300 (1966).

[7] K. N. G. Fuller and D. Tabor, Proc. R. Soc. London, Ser. A **345**, 327 (1975).

[8] K. L. Johnson, K. Kendall, and A. D. Roberts, Proc. R. Soc. London, Ser. A **324**, 301 (1971).

[9] B. N. J. Persson, Eur. Phys. J. E **8**, 385 (2002).

[10] S. Zilberman and B. N. J. Persson, Solid State Commun. **123**, 173 (2002).

[11] S. Zilberman and B. N. J. Persson, Solid State Commun. **124**, 227 (2002).

[12] S. Zilberman and B. N. J. Persson, J. Chem. Phys. **118**, 6473 (2003).

[13] B. N. J. Persson and E. Tosatti, J. Chem. Phys. **115**, 5597 (2001).

[14] B. N. J. Persson, Phys. Rev. Lett. **89**, 245502 (2002).

[15] B. N. J. Persson, Wear **254**, 832 (2003).

[16] B. N. J. Persson, J. Chem. Phys. **118**, 7614 (2003).

[17] B. N. J. Persson and S. Gorb, J. Chem. Phys. **119**, 11437 (2003).

[18] K. Kendall, *Molecular Adhesion and its Applications: The Sticky Universe* (Kluwer Academic, Dordrecht, 2001).

[19] H. Yoshizawa, Y.-L. Chen, and J. Israelachvili, J. Phys. Chem. **97**, 4128 (1993).

[20] B. N. J. Persson and P. Ballone, Solid State Commun. **115**, 599 (2000).

[21] B. N. J. Persson and P. Ballone, J. Chem. Phys. **112**, 9524 (2000).

[22] B. N. J. Persson, V. N. Samoilov, S. Zilberman, and A. Nitzan, J. Chem. Phys. **117**, 3897 (2002).

[23] B. N. J. Persson, O. Albohr, F. Mancosu, V. Peveri, V. N. Samoilov, and I. M. Sivebaek, Wear **254**, 835 (2003).

[24] I. M. Sivebaek, V. N. Samoilov, and B. N. J. Persson, J. Chem. Phys. **119**, 2314 (2003).

[25] I. M. Sivebaek, V. N. Samoilov, and B. N. J. Persson, Tribol. Lett. **16**, 195 (2004).

[26] I. M. Sivebaek, S. C. Sorensen, J. Jakobsen, B. N. J. Persson, and V. N. Samoilov, Soc. Automot. Eng. [Spec. Publ.] SAE Tech. Paper 2003-01-3286 (2003).

[27] V. N. Samoilov and B. N. J. Persson, J. Chem. Phys. **120**, 1997 (2004).

[28] U. Landman, W. D. Luedtke, and E. M. Ringer, Wear **153**, 3 (1992).

[29] U. Landman, W. D. Luedtke, J. Ouyang, and T. K. Xia, Jpn. J. Appl. Phys. **32**, 1444 (1993).

[30] U. Landman and W. D. Luedtke, Appl. Surf. Sci. **92**, 237 (1996).

[31] J. Gao, W. D. Luedtke, and U. Landman, J. Chem. Phys. **106**, 4309 (1997).

[32] J. Gao, W. D. Luedtke, and U. Landman, J. Phys. Chem. B **101**, 4013 (1997).

[33] S. T. Cui, P. T. Cummings, and H. D. Cochran, J. Chem. Phys. **114**, 7189 (2001).

[34] M. L. Gee, P. M. McGuiggan, J. N. Israelachvili, and A. M. Homola, J. Chem. Phys. **93**, 1895 (1990).

[35] J. P. Gao, W. D. Luedtke, and U. Landman, Phys. Rev. Lett. **79**, 705 (1997).

[36] H. Tamura, M. Yoshida, K. Kusakabe *et al.*, Langmuir **15**, 7816 (1999).

[37] A. L. Demirel and S. Granick, Phys. Rev. Lett. **77**, 2261 (1996).

[38] A. L. Demirel and S. Granick, J. Chem. Phys. **109**, 6889 (1998).

[39] J. Klein and E. Kumacheva, Science **269**, 816 (1995).

[40] E. Kumacheva and J. Klein, J. Chem. Phys. **108**, 7010 (1998).

[41] B. N. J. Persson and E. Tosatti, Phys. Rev. B **50**, 5590 (1994).

[42] B. N. J. Persson, Chem. Phys. Lett. **324**, 231 (2000).

[43] W. L. Jorgensen, J. D. Madura, and C. J. Swenson, J. Am. Chem. Soc. **106**, 6638 (1984).

[44] D. K. Dysthe, A. H. Fuchs, and B. Rousseau, J. Chem. Phys. **112**, 7581 (2000).

[45] T. K. Xia, J. Ouyang, M. W. Ribarsky, and U. Landman, Phys. Rev. Lett. **69**, 1967 (1992).

[46] J. Rottler and M. O. Robbins, J. Adhes. Sci. Technol. **17**, 369 (2003).